

BUNCH COMPRESSION MONITOR BASED ON COHERENT DIFFRACTION RADIATION AT EUROPEAN XFEL AND FLASH

Ch. Gerth* and N. M. Lockmann
 Deutsches Elektronen-Synchrotron, Hamburg, Germany, EU

Abstract

Bunch compression monitors (BCMs) based on the detection of coherent diffraction radiation have been installed at the European XFEL for a beam-based stabilisation of the accelerating phases as well as monitoring of bunch lengths. The monitor systems comprise zero-bias Schottky and pyro-electric detectors in combination with low and high pass filters. The detector responses and filters are matched to the spectral ranges of the coherent part of the emitted diffraction radiation which is given by the particular beam energy and bunch lengths after each bunch compression stage. In this paper, we describe in detail the experimental setup of the BCMs. The last BCM has been calibrated with the help of a transverse deflecting structure to establish a (rms) bunch length monitor in the range of a few tens of femtoseconds, and results from compression scans are presented. To enable operation at megahertz repetition rates of the superconducting accelerator, a correction method for the signal pileup of the pyro-electric detectors has been applied. Installation of the same BCMs is foreseen at FLASH within the FLASH2020+ upgrade project.

EUROPEAN XFEL

High-gain, single-pass free-electron lasers (FELs) require high-brightness electron bunches with kiloampere peak currents, which are longitudinally compressed in several stages by off-crest acceleration in combination with magnetic dipole chicanes. Figure 1 depicts schematically an overview of the European XFEL accelerator [1] with three radio-frequency (RF) accelerating sections (L_1, L_2, L_3) followed by bunch compression chicanes (BC_1, BC_2, BC_3). The settings of the compression stages were optimised for various bunch charges [2] as the electron bunches can be affected by collective, non-linear effects at these high peak currents. To establish the correct compression settings and ensure stable, long-term FEL operation, monitoring of the bunch compression is mandatory.

Bunch compression monitors (BCM) based on the detection of coherent diffraction radiation (CDR) have been installed after each of the three BC chicanes as is indicated in Fig. 1. CDR is generated by an electron bunch passing through an aperture in a screen and, therefore, is non-invasive to the electron beam. BCM1 has been installed after L_2 at higher beam energies, as this leads to a smaller emittance and, therewith, beam size and reduces the risk of beam losses at the aperture.

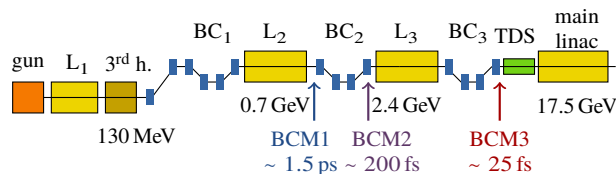


Figure 1: Schematic overview of the European XFEL accelerator. The positions of the BCs and nominal rms bunch lengths for a bunch charge of 250 pC are indicated.

BCM SETUP

A BCM consists of a screen station mounted in the electron beamline for the generation of CDR as well as an optics and detector unit for transport and detection of the CDR.

Screen Station

Figure 2 shows a CAD image of the screen station and CDR screen which is mounted on a remotely-controllable vacuum feed-through (screen mover). The screen consists of solid aluminum, and the screen normal has an angle of 45° with respect to the electron beam axis. The radiator area at the bottom ($32 \text{ mm} \times 80 \text{ mm}$, 1 mm-thick) is depicted enlarged in the right part of Fig. 2 and comprises two apertures with effective diameters of 5 mm and 7 mm in the projection of the electron beam axis. The surface of the CDR screen has been machined with a diamond milling cutter and has a roughness $< 1 \mu\text{m}$. Backward CDR is emitted perpendicular to the electron beam axis and enters the optics and detector unit through a fused silica vacuum window at BCM1 and BCM2 and a diamond vacuum window at BCM3.

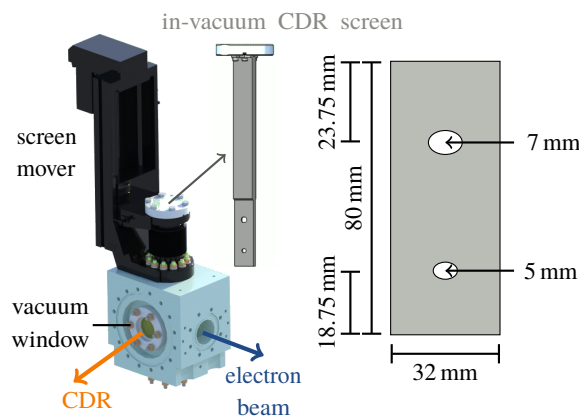


Figure 2: (Left) CAD model of the screen station and CDR screen. (Right) The radiator area enlarged with dimension.

* christopher.gerth@desy.de

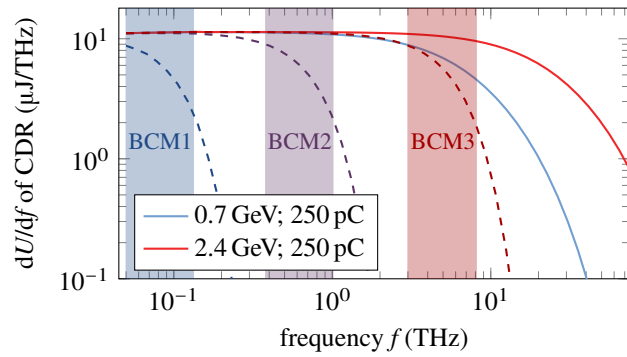


Figure 3: Spectral energy density emitted by the CDR screen (aperture $\Phi = 7$ mm) at beam energies of 0.7 GeV (solid blue) and 2.4 GeV (solid red). The dashed lines include the form factor term $|F(f)|^2$ of Eq. (1) and are calculated for Gaussian longitudinal profiles with rms bunch lengths as given in Fig. 1. The coloured areas mark the regions where the form factor term decreases from 0.8 to 0.2.

The spectral energy density of CDR emitted at the screen station scales quadratically with the bunch charge Q and can be expressed by

$$\left[\frac{dU}{df} \right]_{\text{CDR}} = \left[\frac{dU}{df} \right]_1 \cdot \left(\frac{Q}{e} \right)^2 \cdot |F(f)|^2, \quad (1)$$

where $[dU/df]_1$ is the spectral energy density emitted by a single electron and $F(f)$ the complex form factor which is described by the 3D-particle distribution of the electron bunch. Transverse beam size effects are strongly suppressed for the frequency ranges and electron beam energies considered here, and $F(f)$ can be approximated by the longitudinal form factor $F_l(f)$ which is given by the Fourier transform of the normalised longitudinal current profile $\rho(t)$:

$$F_l(f) = \int_{-\infty}^{+\infty} \rho(t) \exp(-i2\pi ft) dt. \quad (2)$$

The spectral energy density has been calculated with the help of the generalised Ginzburg-Frank equation for DR given in Ref. [3] for infinitesimally short electron bunches at a beam energy of 0.7 GeV (solid blue line, BCM1 and BCM2) and 2.4 GeV (solid red line, BCM3) and is depicted in Fig. 3. CDR has the advantage of being non-invasive, however, the spectral energy density exhibits a cut-off towards high frequencies depending on the beam energy. The dashed lines include the longitudinal form factor $F_l(f)$ for electron bunches that have a Gaussian current profile with rms bunch lengths as indicated in Fig. 1. The coloured areas mark the frequency regions where the form factor term $|F(f)|^2$ in Eq. (1) decreases from 0.8 to 0.2. The latter are of interest for the BCM, as bunch length changes lead to strong variations of the radiated energy in these frequency bands, while radiated energies at lower (DC content) or higher (sub-structures) frequencies do not contain any information on changes of the rms bunch length.

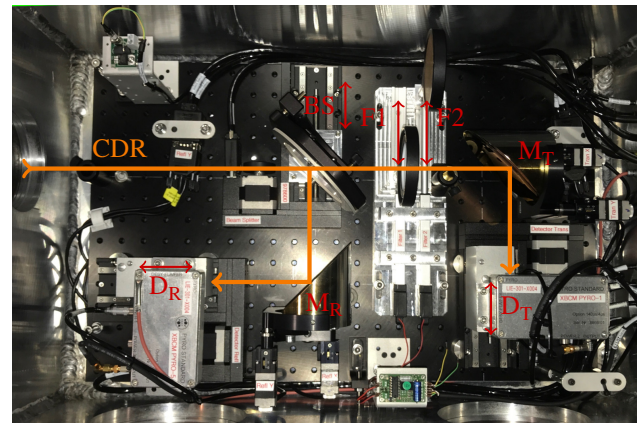


Figure 4: Photograph showing a top view of the optics and detector unit. The beam path and components are marked (BS: beamsplitter, F: filter, M: mirror, D: detector).

Optics and Detector Unit

A photograph showing a top view of the compact optics and detector unit is depicted in Fig. 4. All components are enclosed in a sealed aluminum housing to be insensitive to humidity changes inside the accelerator tunnel. The housing can be attached directly to the supports of the electron beamline, which is suspended at a height of 2.25 m. All optical components are mounted with commercially available supports onto a solid aluminum breadboard with a footprint of 600×400 mm².

The first optical element is a thin film polarizer used as beamsplitter (BS, $\Phi = 4''$, Microtech Instruments, F15-L) that separates the radial polarised CDR into a transmitted (vertically polarised) and reflected (horizontally polarised) beam path. By retracting the beamsplitter out of the beam path, the full CDR intensity is transported into the transmitted beam path. The transmitted beam path is equipped with two filter holders (F1 and F2, $\Phi = 3''$, angle = 90°) which can be moved independently. The CDR is then focused by gold-coated toroidal mirrors (M_T and M_R , $\Phi = 3''$, LT Ultra) with a focal length of 101.6 mm onto the detectors (D_T and D_R). The mirrors are adjustable to compensate misalignments of the experimental setup, and the detectors are mounted on linear stages to be able to move longitudinally through the focus. In order to match the respective frequency range (see Fig. 3), zero-bias Schottky diodes (75 - 100 GHz, DET-10-RPFWO, Millitech) are used at BCM1 and pyro-electric detectors (DESY in-house) at BCM2 and BCM3. The detector signals are transmitted by coaxial cables of several meters length to a digitizer board (SIS8300-L2D, Struck Innovative Systeme) in MicroTCA.4 standard, which is the common front-end electronics of the European XFEL accelerator.

BCM CALIBRATION

A cross-calibration of the BCM signal to rms bunch lengths has been established with the help of a TDS [4] for the last BCM (see Fig. 1) where the electron bunches are fully compressed. As was demonstrated in Ref. [5],

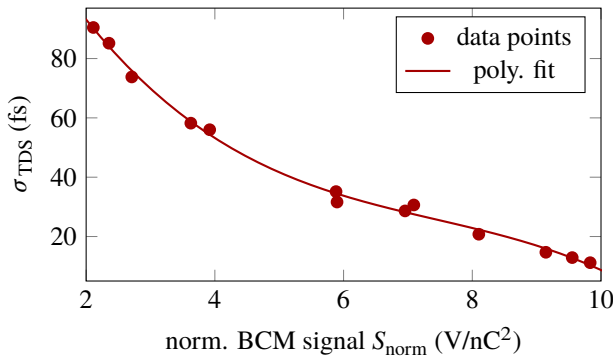


Figure 5: Third-order polynomial fit (solid line) as a cross-calibration of the charge-normalised BCM signal S_{norm} to the rms bunch lengths σ_{TDS} measured with a TDS.

the particular shape of the longitudinal profiles of electron bunches with the same rms bunch length leads to differences in the form factor $F(f)$ at high frequencies. Therefore, a low-pass filter with a cut-off frequency of 6 THz was applied (see Fig. 3). Furthermore, as the CDR intensity and thereby BCM signal S_{BCM} scales quadratically with the bunch charge Q (see Eq. (1)), the normalised BCM signal $S_{\text{norm}} = S_{\text{BCM}}/Q^2$ has to be considered.

The cross-calibration has been obtained for a bunch charge $Q = 250$ pC by varying compression settings of the accelerator modules L_2 and L_3 (see Fig. 1) and, therewith, the bunch lengths between 6 fs and 90 fs. The result is shown in Fig. 5 where the rms bunch lengths measured with the TDS (red dots) are plotted vs. the charge-normalised BCM signal together with a third-order polynomial fit (solid line). For the determination of the rms bunch lengths, the temporal resolution R_{TDS} of the TDS has been subtracted quadratically according to

$$\sigma_{\text{TDS}} = \sqrt{\sigma_{\text{mess}}^2 - R_{\text{TDS}}^2} . \quad (3)$$

The same set of data is plotted in Fig. 6 for the independent compression scans of L_2 (top) and L_3 (bottom), for which the RF amplitude and phase of the accelerating fields were varied such that the mean beam energy remained constant. The rms bunch lengths measured with BCM3 were determined with the use of the third-order polynomial fit in Fig. 5. The relative difference between the rms bunch lengths measured with the TDS (green dots) and determined from BCM data (red line) is less than 10%. However, the long-term validity of the BCM3 calibration with the third-order polynomial fit needs to be confirmed in further comparative measurements and probably established separately for operation at different bunch charges.

MEGAHERTZ OPERATION

The superconducting accelerator of European XFEL delivers bunch trains of up to $600 \mu\text{s}$ at a repetition rate of 10 Hz with an intra-train rate of up to 4.5 MHz. By using non-invasive CDR and fast detection systems in combination

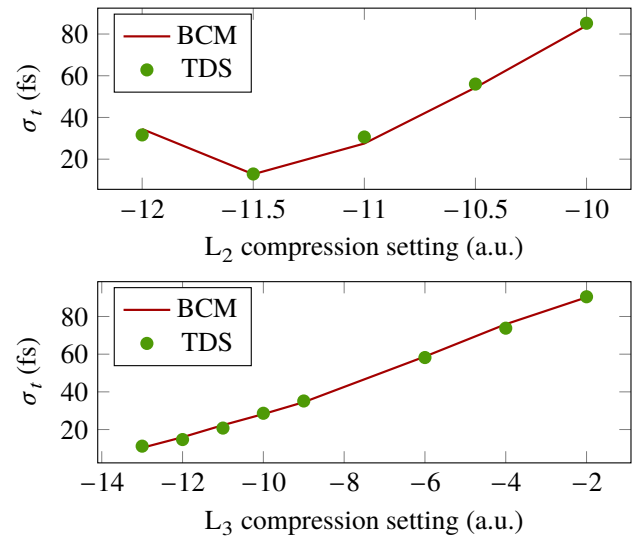


Figure 6: Comparison of rms bunch lengths measured with the TDS and obtained from the BCM data with the calibration presented in Fig. 5.

with the BCM calibration described above, determination of the rms bunch lengths along the bunch trains can be realised in parallel to FEL user operation. However, mechanical oscillations of the pyro-electric detectors with characteristic frequencies in the vicinity of the bunch repetition rate lead to signal pileup which needs to be corrected.

Signal Pileup Correction

The influence of the pileup effect on the BCM signals is demonstrated in Fig. 7 for a bunch train that was sampled with the ADC (blue curve) at a bunch repetition rate of 4.5 MHz. For the first ≈ 50 bunches a signal slope is induced, while for later bunches the signal pileup evolves into a constant contribution. After the last bunch there is no CDR emitted, however, pileup results in a non-zero signal. An algorithm to correct the pileup in the signal processing

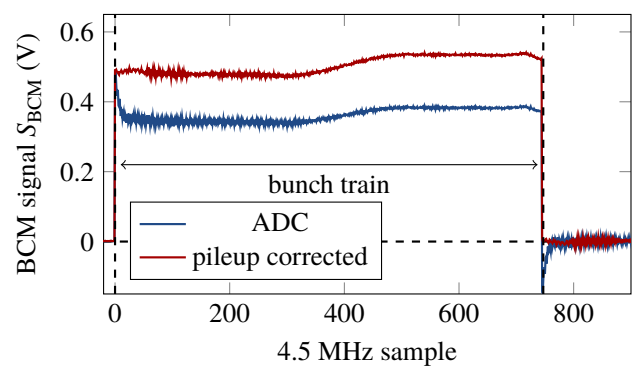


Figure 7: Example of signal pileup (blue) sampled with the ADC at a bunch repetition rate of 4.5 MHz. The bunch train begins at sample #0 and ends at #750. Pileup leads to artificial signal slopes at the beginning and after the bunch train, which are removed by applying pileup correction (red).

has been presented in Ref. [6] and is applied routinely to the BCMs equipped with pyro-electric detectors. In comparison to the raw ADC signal, for the pileup corrected signal (red curve) the slope of the first bunches is removed and the baseline after the bunch train is zero within the noise level.

Comparative Measurements with TDS

Compression data has been recorded with BCM3 during operation with 1.1 MHz bunch repetition rate. The signals have been pileup corrected and converted into rms bunch lengths σ_r by applying the calibration with the TDS as described above. The resulting mean of the rms bunch lengths for 30 bunch trains (red curve) is presented in Fig. 8 together with the rms fluctuations as an error band (light red).

The measured rms bunch lengths increase continuously along the first 90 bunches with a steep slope beginning at bunch #60. Afterwards, the BCM signal remains approximately constant until the end of the bunch train at bunch #390. During this measurement, the RF accelerating parameters for bunch compression were divided into two different settings along the bunch train, and these so-called RF flattops are marked as FT1 and FT2 in Fig. 8. This operation mode enables operation of two FEL beamlines in parallel with independently optimised compression settings. The transition time between the RF flattops is required for adjustment of the RF parameters in the superconducting accelerator.

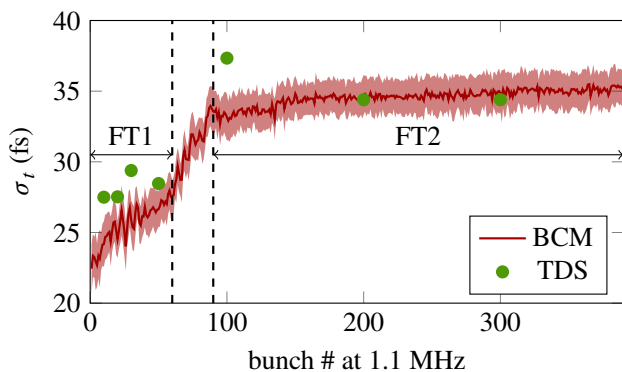


Figure 8: Bunch lengths (rms) measured for all bunches in the bunch train with BCM3 (red curve) by applying the calibration presented in Fig. 5 and for a few selected bunch numbers with the TDS (green dots). The solid red line represents the mean of 30 consecutive bunch trains.

The difference in bunch compression for both RF flattops is clearly detected by the BCM, and the transition between both RF flattops at bunch numbers #60 to #90 exhibits a steep increase of the rms bunch length by about 7 fs. This behaviour of the rms bunch lengths is confirmed by comparative measurements with the TDS in combination with a fast kicker magnet and off-axis screen [4]. The rms bunch lengths have been measured successively for a few selected bunch numbers, and the temporal resolution of about 15 fs

has been corrected according to Eq. (3). The TDS results (green dots) are compared to the BCM data in Fig. 8 and show good overall agreement and corroborate the increase in bunch length in RF flattop FT1 and constant behaviour in flattop FT2. The relative deviations for the rms bunch lengths obtained with BCM and TDS are less than 15%.

CONCLUSIONS

BCMs have been installed after each bunch compressor at European XFEL to measure the bunch compression non-invasively during FEL operation for optimisation and stabilisation of the superconducting linear accelerator. A signal pileup correction has been implemented for the pyro-electric detectors to enable bunch-resolved measurements at intra-train repetition rates of up to 4.5 MHz. Based on a successful calibration with a TDS, the signals of the BCM after the last bunch compressor are converted to rms bunch lengths which allows monitoring of entire bunch trains. BCMs with the same layout will be installed at FLASH within the framework of the FLASH2020+ Upgrade Project [7].

ACKNOWLEDGEMENTS

The authors would like to thank O. Hensler and R. Kammering for their support with BCM control software and B. Beutner for his assistance with the TDS measurements.

REFERENCES

- [1] W. Decking *et al.*, “A MHz-repetition-rate hard X-ray free-electron laser driven by a superconducting linear accelerator,” *Nature Photonics*, vol. 14, no. 6, pp. 391–397, 2020. doi: 10.1038/s41566-020-0607-z.
- [2] I. Zagorodnov, M. Dohlus, and S. Tomin, “Accelerator beam dynamics at the european x-ray free electron laser,” *Phys. Rev. Accel. Beams*, vol. 22, p. 024401, 2 2019. doi: 10.1103/PhysRevAccelBeams.22.024401.
- [3] S. Casalbuoni, B. Schmidt, and P. Schmüser, “Far-infrared transition and diffraction radiation, part I: Production, diffraction effects and optical propagation,” DESY, Hamburg Germany, Report 2005-15, 2005.
- [4] C. Gerth, B. Beutner, O. Hensler, F. Obier, M. Scholz, and M. Yan, “Online longitudinal bunch profile and slice emittance diagnostics at the European XFEL,” 2017, pp. 153–156. doi: 10.18429/JACoW-IBIC2017-TUPCC03.
- [5] M. Veronese, R. Appio, P. Craievich, and G. Penco, “Absolute bunch length measurement using coherent diffraction radiation,” *Phys. Rev. Lett.*, vol. 110, p. 074802, 7 2013. doi: 10.1103/PhysRevLett.110.074802.
- [6] N. M. Lockmann, C. Gerth, B. Schmidt, and S. Wesch, “Non-invasive THz spectroscopy for bunch current profile reconstructions at MHz repetition rates,” *Phys. Rev. Accel. Beams*, vol. 23, p. 112801, 11 2020. doi: 10.1103/PhysRevAccelBeams.23.112801.
- [7] E. Allaria *et al.*, “FLASH2020+ plans for a new coherent source at DESY,” in *Proc. IPAC’21*, TUPAB086, Campinas, SP, Brazil, 2021.